Electroweak di-boson production in ATLAS

Johannes Ebke

Ludwig-Maximilians-Universität München

on behalf of the ATLAS Collaboration

7 June 2011

Physics at the LHC 2011

Outline

Outline

The ATLAS Detector

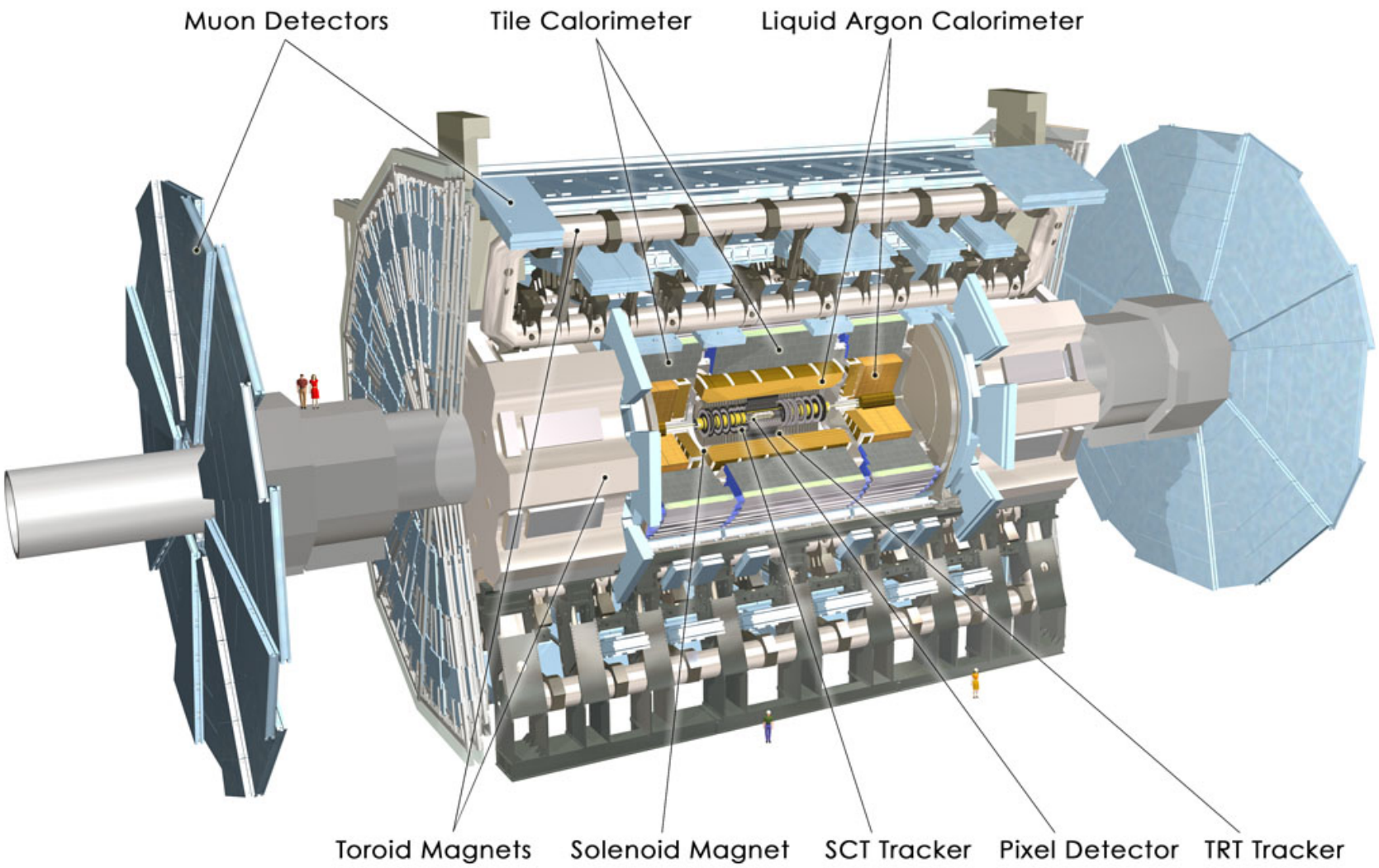

Measurement of differential $\gamma\gamma$ cross-section

ATLAS-STDM-2011-05-001

Data

- Using the complete ATLAS dataset for 2010 with $\sqrt{s} = 7$ TeV, corresponding to 37.2 pb^{-1}

Overview

- Primary production: $q\bar{q}/gg \to \gamma\gamma$
- Higher orders $q\bar{q}/gg \to g\gamma\gamma$ and $qg \to q\gamma\gamma$
- Sensitive to double fragmentation at small $\Delta\varphi_{\gamma\gamma}$
- Irreducible background for some new physics searches, such as the $H \to \gamma\gamma$ search

Main Backgrounds

- Hadronic jets - controlled by isolation transverse energy
- Misidentified electrons (mostly conversions) - controlled by measuring misID rate at the Z peak

Measurement of differential $\gamma\gamma$ cross-section

Selection

- Require two "tight" photons with
  - transverse momentum $p_T^{\gamma} > 16$ GeV
  - and $|\eta^{\gamma}| < 2.37$
  - ..but excluding $1.37 < |\eta^{\gamma}| < 1.52$ (barrel-endcap transition)
- The separation of the two photons must be $\Delta R_{\gamma\gamma} > 0.4$
- Both photons must be isolated: The transverse isolation $E_T^{iso} < 3$ GeV

Isolation transverse energy

\+ sum ECAL and HCAL cells surrounding the photon

\- subtract central core with most of the photon E_T

% correct out-of-core energy

\- subtract ambient energy correction from soft jets and in-time pileup

Details of the two-dimensional Fit

Method

Require two "tight" photons. Fit ($E_{T,1}^{iso}$, $E_{T,2}^{iso}$) with distributions derived from non-tight/tight and non-tight/non-tight samples.

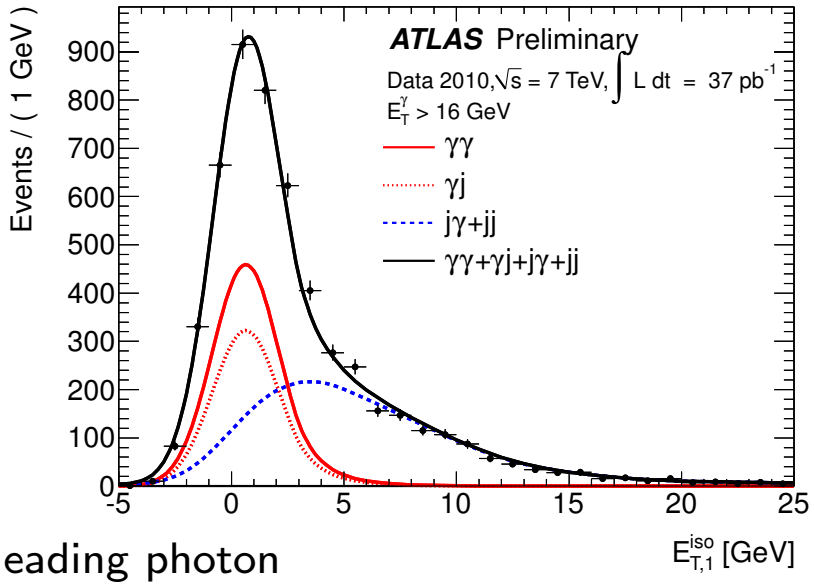

leading photon

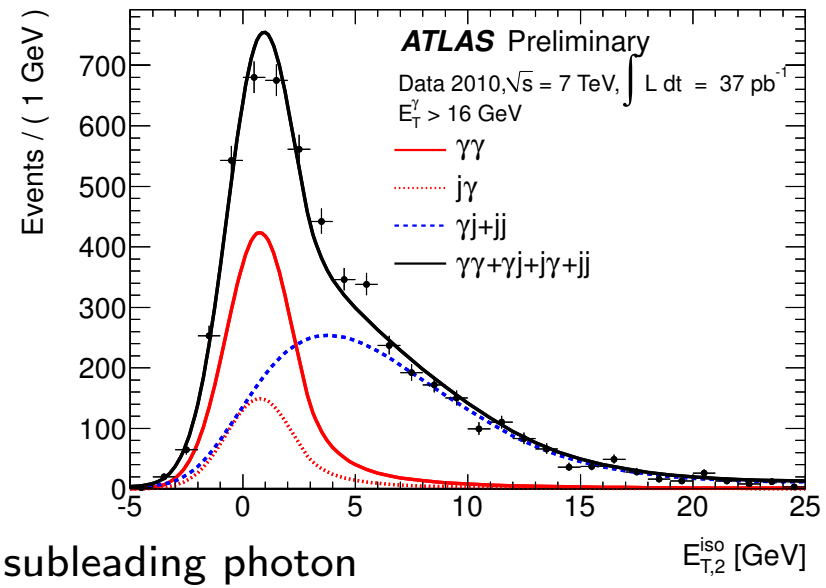

subleading photon

Projections of the 2-dimensional PDF fit onto the transverse isolation energy E_T^{iso} of each photon candidate

Jet Background Substraction

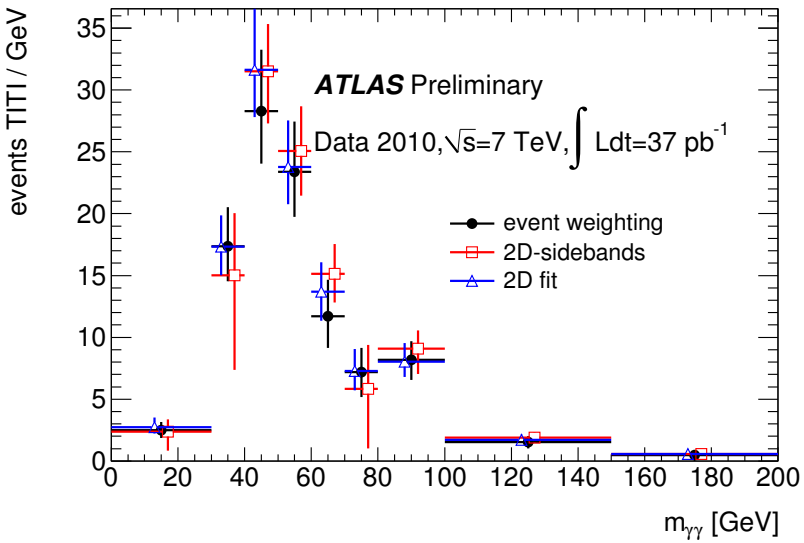

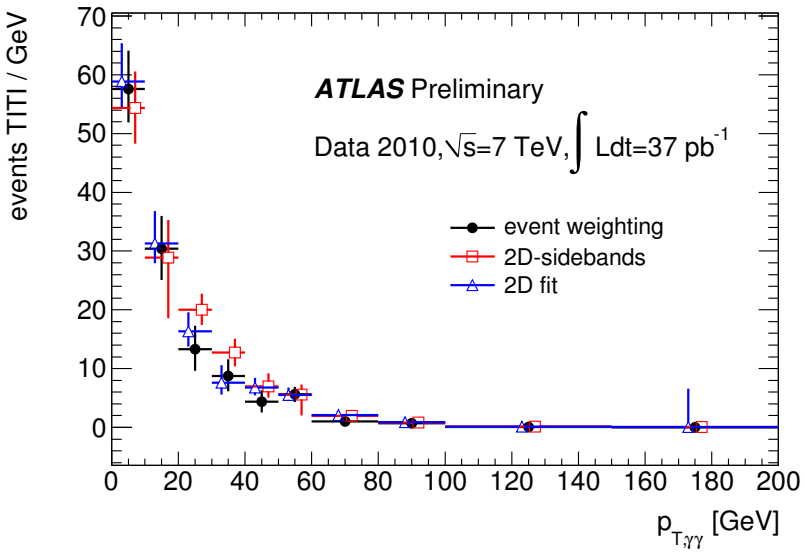

Subtraction Methods

- Reweighting using fake/efficiency matrix
- Two-dimensional fit of leading/subleading isolation energy
- 2D Sideband counting

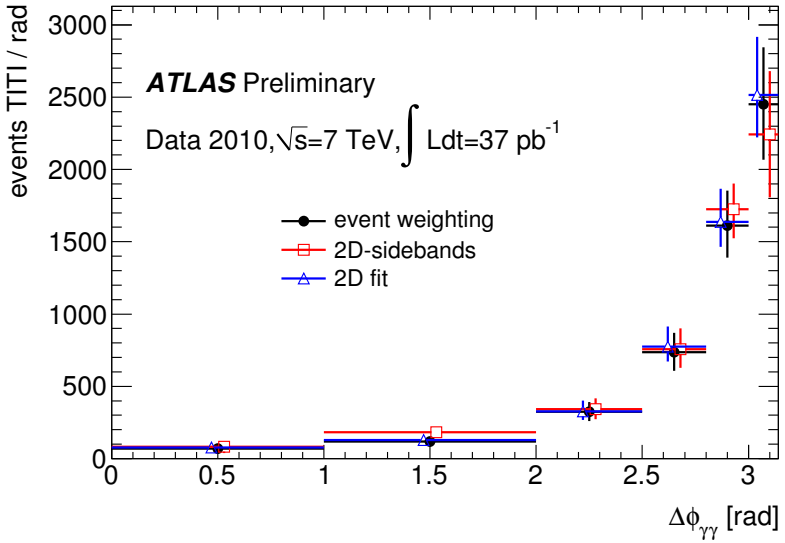

Differential cross-section $d\sigma/dm_{\gamma\gamma}$

Error bars

The error bars show the total uncertainty, the statistical contribution is marked in red.
The hatched bands display the NLO computations by DIPHOX and ResBos.

Conclusion

Good agreement with both predictions, except in low mass region - related to $\Delta\varphi_{\gamma\gamma}$ discrepancy.

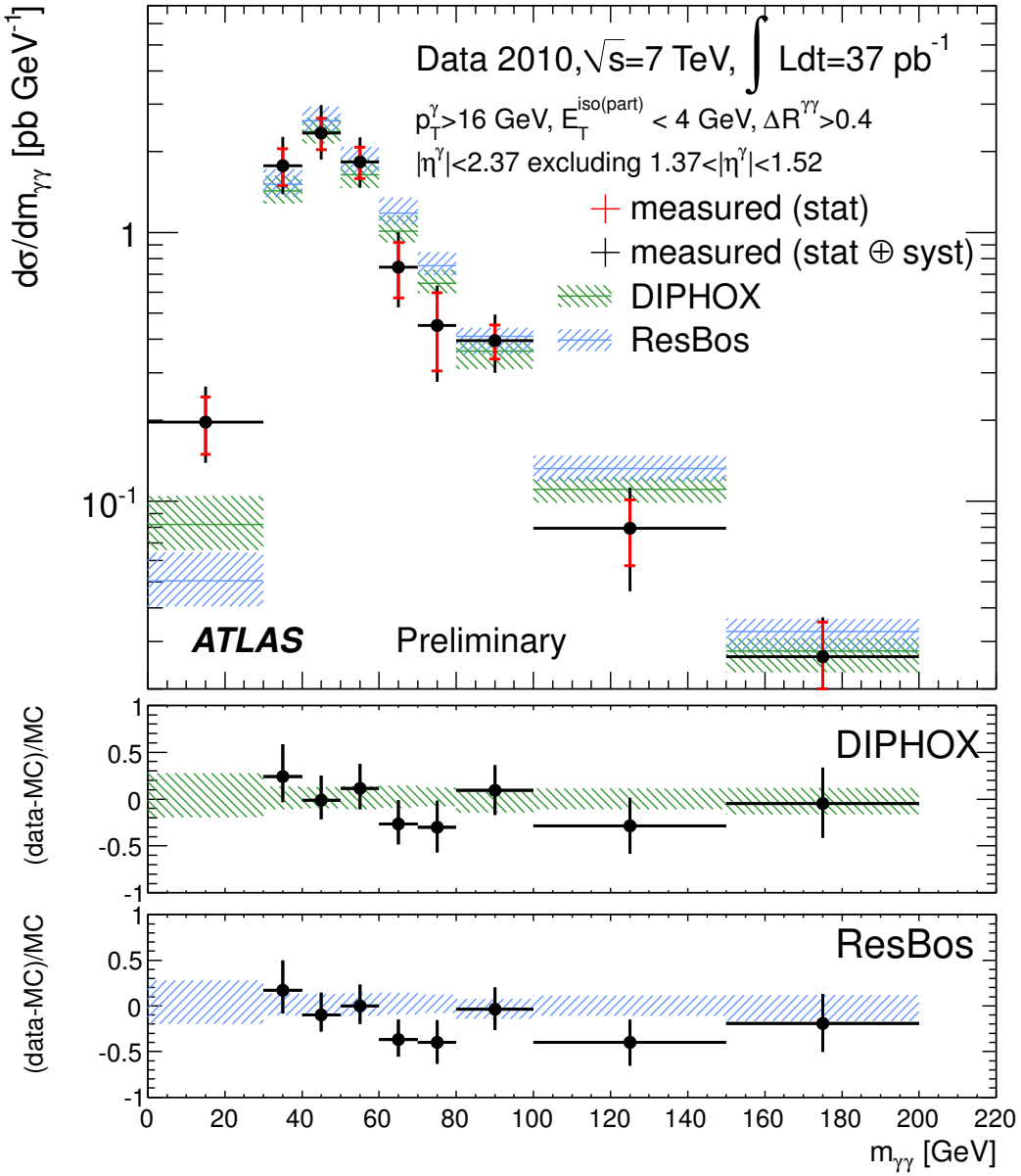

Differential XSs $d\sigma/dp_{T_{\gamma\gamma}}$ and $d\sigma/d\Delta\varphi_{\gamma\gamma}$

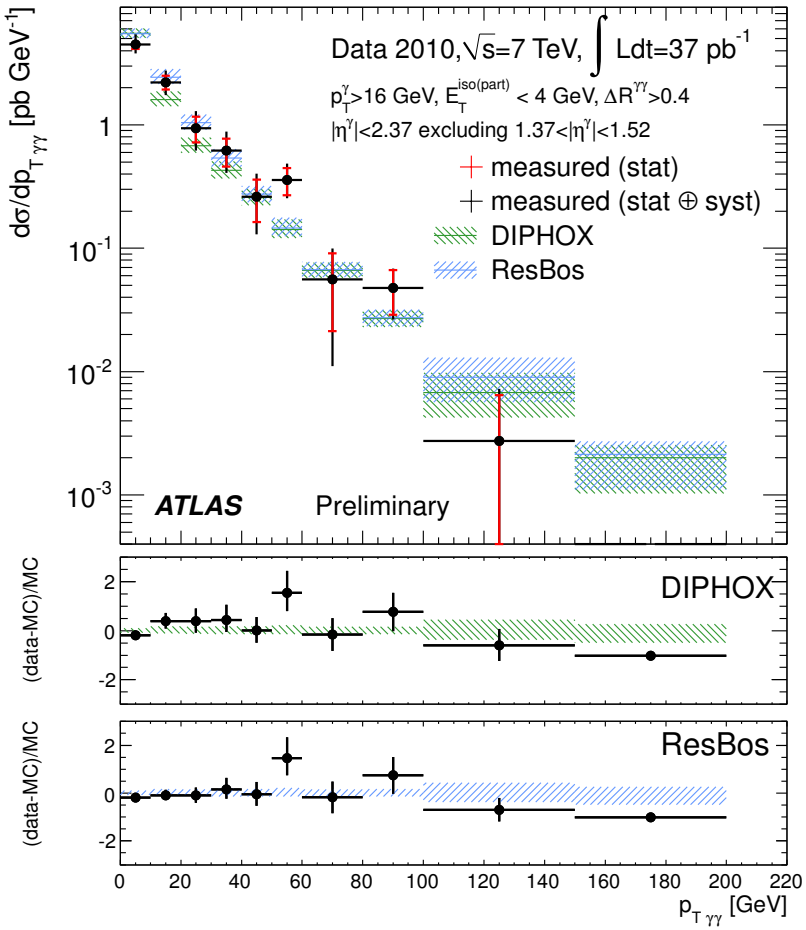

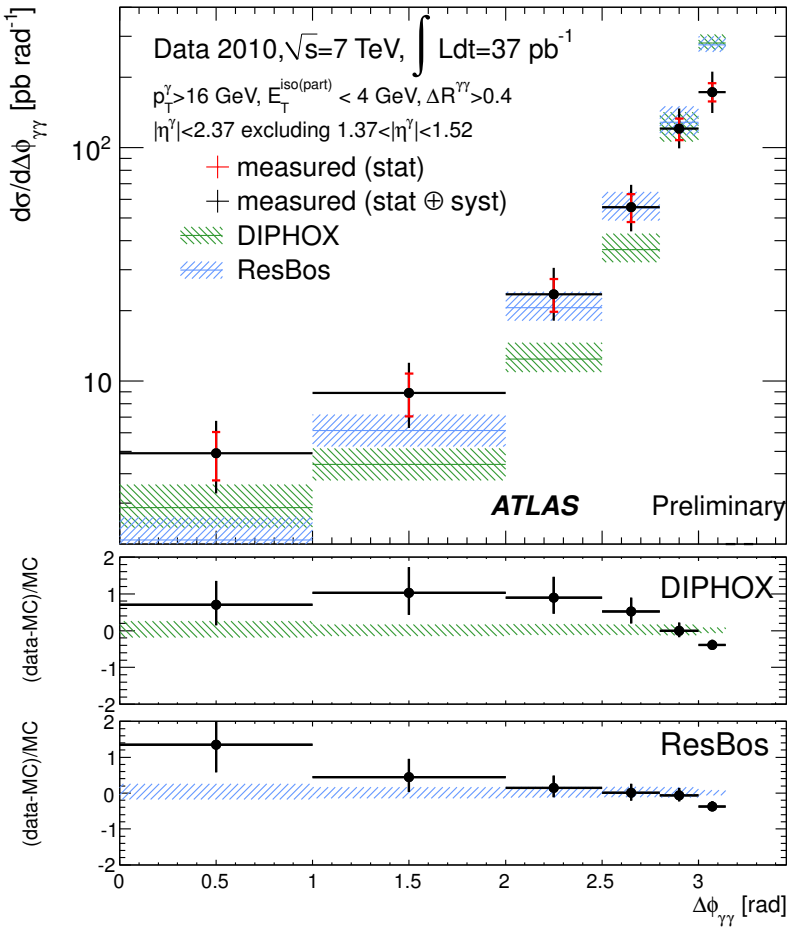

Conclusion

Generally good agreement with both predictions, except in the region between 50 GeV and 60 GeV

Conclusion

Spectrum broader towards low values of $\Delta\varphi_{\gamma\gamma}$ than NLO predictions. Similar effects also observed at the TeVatron.

$W\gamma/Z\gamma$ PRODUCTION DIAGRAMS

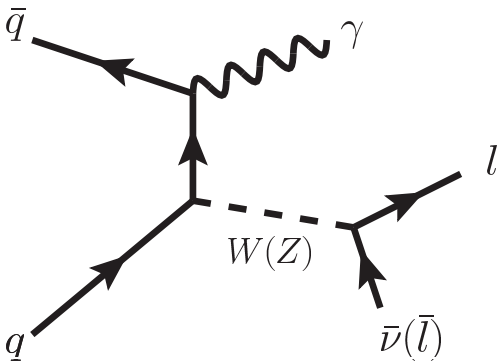

u-channel

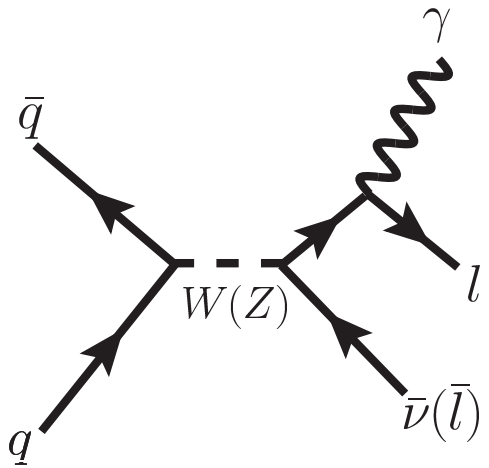

FSR

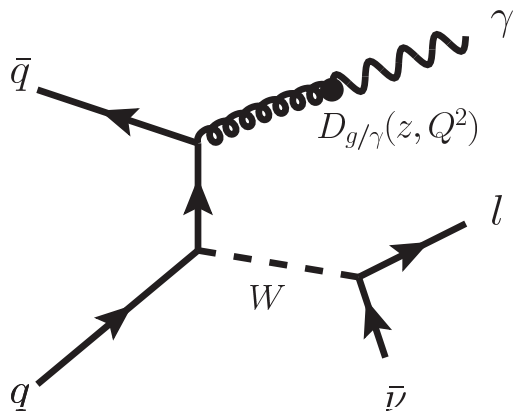

fragmentation

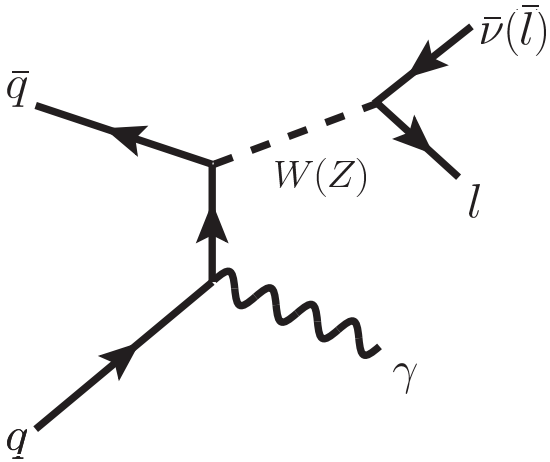

t-channel

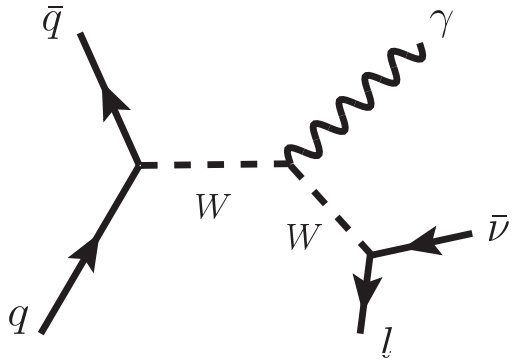

s-channel

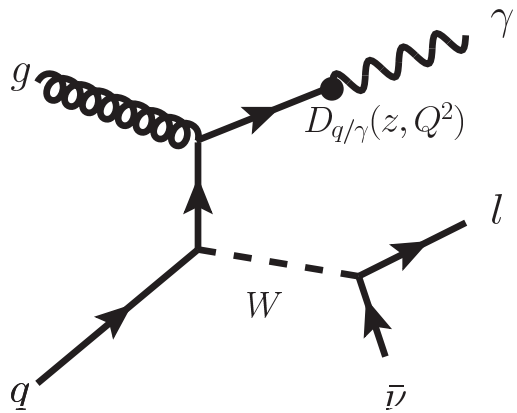

fragmentation

Measurement of the $Z\gamma/W\gamma$ cross-section

ATLAS-STDM-2011-17-002

Data

- Using ATLAS data recorded in 2010 with $\sqrt{s} = 7$ TeV corresponding to 35 pb^{-1}

Selection cuts

- Single electron or muon trigger
- Selection follows closely the W and Z cross-section analyses
- One high p_T Photon $E_T > 15$ GeV
- $\Delta R(l, \gamma) > 0.7$ to suppress FSR contribution

$W\gamma$

- Isolated e or μ
- Large $E_T^{miss} > 25$ GeV
- lepton-E_T^{miss} transverse mass > 40 GeV

$Z\gamma$

- Isolated ee or $\mu\mu$
- Small E_T^{miss}
- dilepton invariant mass > 40 GeV

Photon Isolation distributions

Photon isolation in $W\gamma$

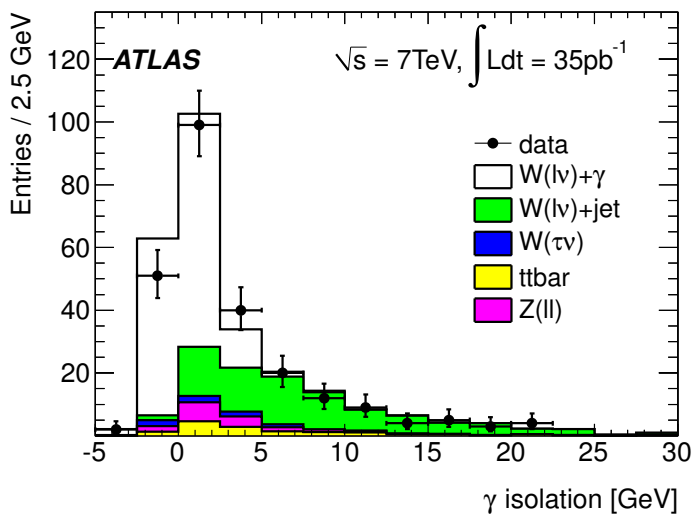

Photon isolation in $Z\gamma$

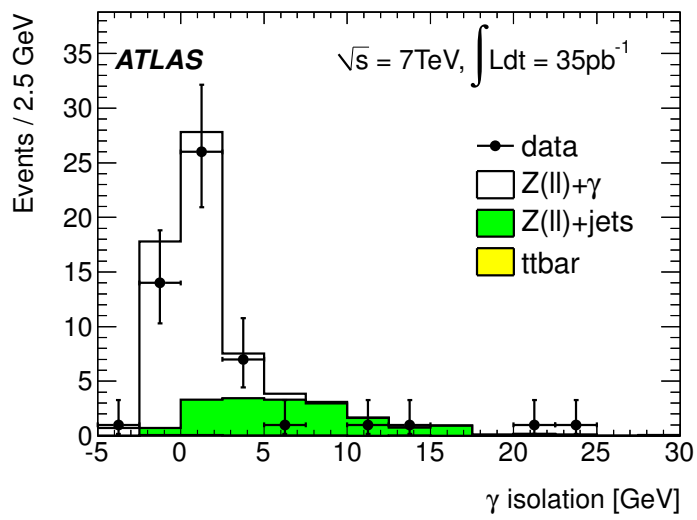

The shape of the predicted W+jets background is taken from the data photon isolation distribution of events in control regions. The normalization is determined by the two-dimensional sideband data-driven method. The predicted contributions from the "EW+tt background" and from the signal are taken from Monte Carlo.

$W\gamma$ and $Z\gamma$ cross-sections

Cross-Sections

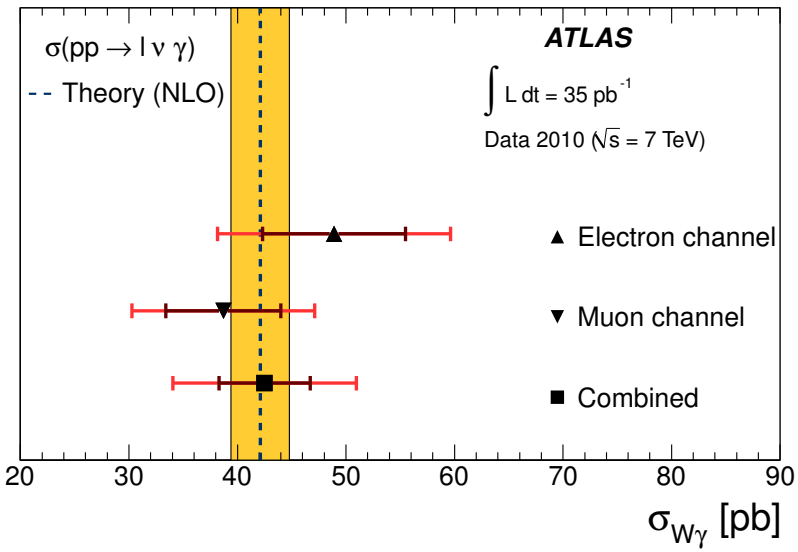

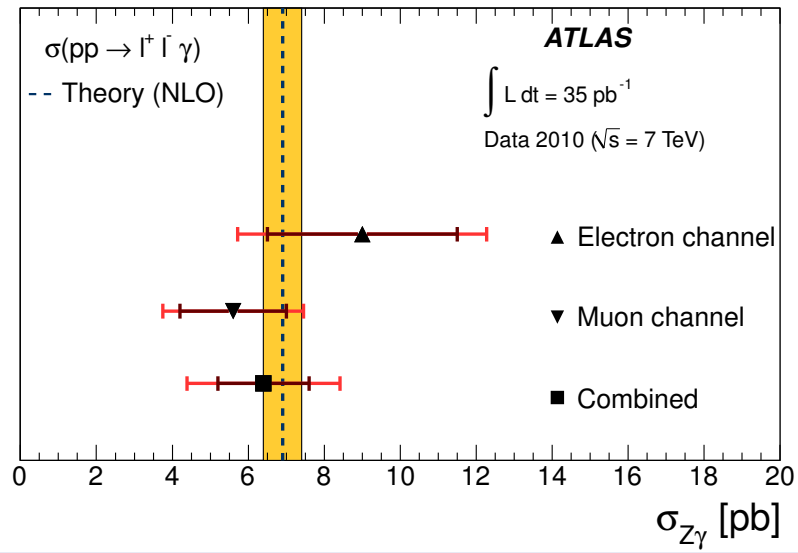

Cross-Section Ratio

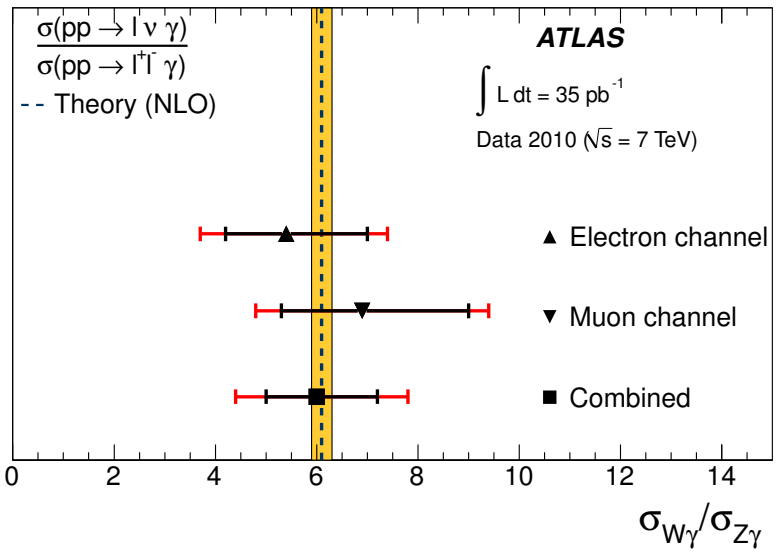

Result

Results of cross-section and cross-section ratio measurements. Good agreement with Standard Model.

Diboson Production Diagrams

WW Production

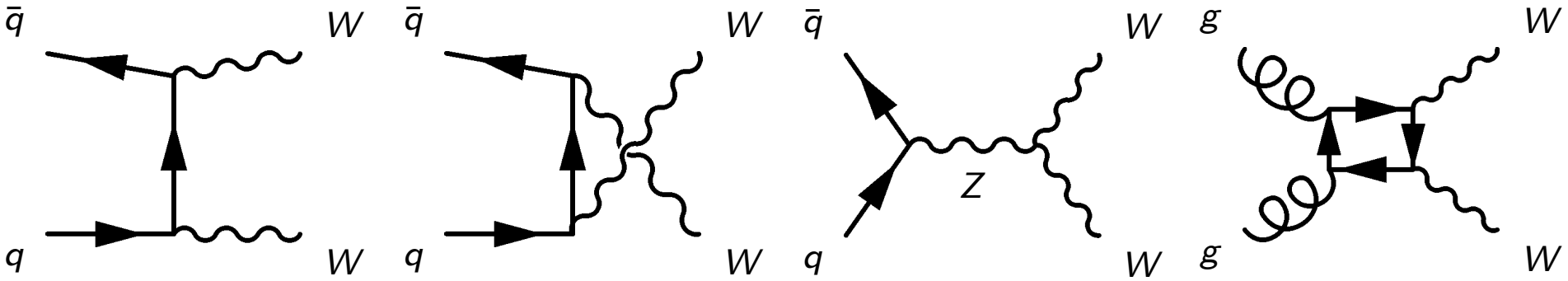

t-channel u-channel s-channel gg-channel

WZ Production

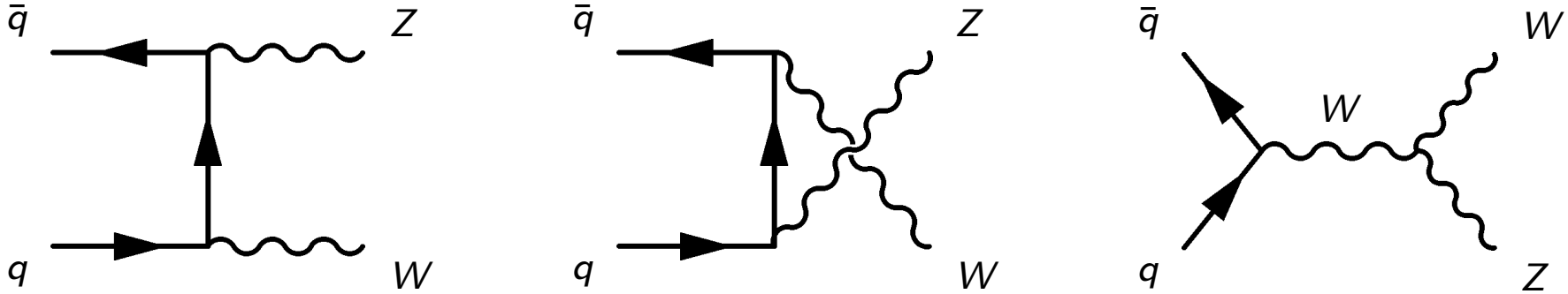

t-channel u-channel s-channel

Measurement of the $W^{\pm}Z$ cross-section

ATLAS-CONF-2011-084

Data

- Data collected in February and May 2011 corresponding to 205 $\text{pb}^{-1} \pm 4.5\%$

Sample selection

- Single electron or muon trigger
- Two leptons with same flavor, opposite sign, and with an invariant mass within 10 GeV of the Zmass
- Additional Lepton
- missing tranverse Energy $E_T^{miss} > 25$ GeV

Main Background: Z+jets and W+jets production

Poster with all the Details!

Look at the Poster from Bernardo Resende for more Details!

Selection

Dilepton Invariant mass

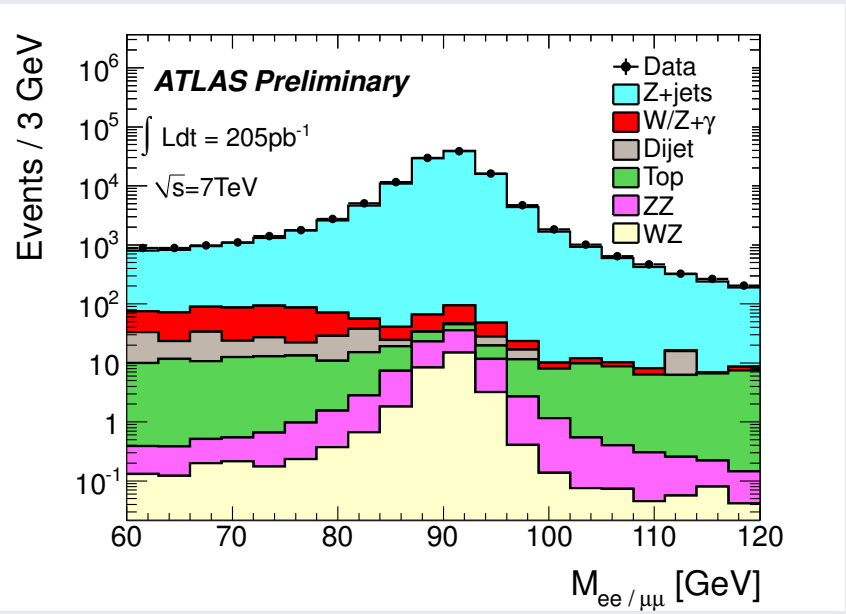

Distribution of m_{ll} of lepton pairs before the Z mass cut

Missing transverse Energy

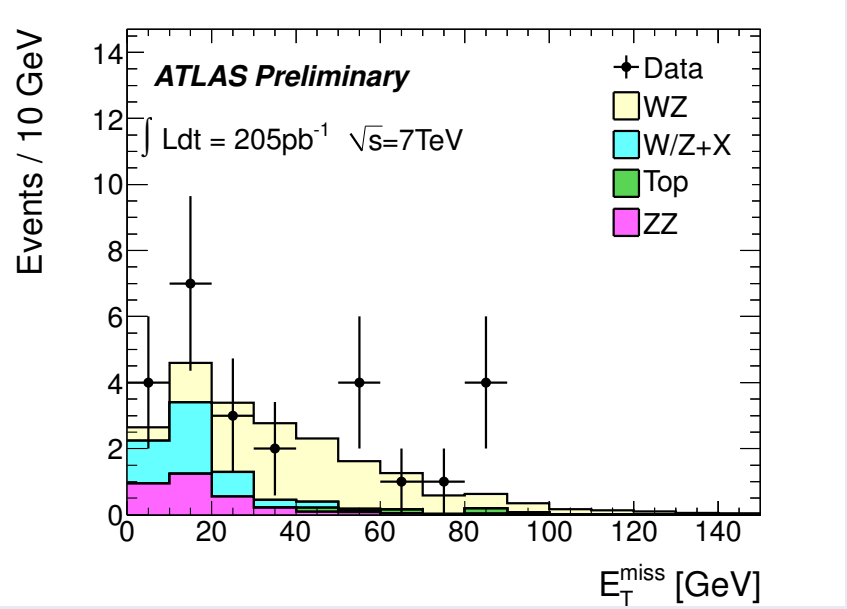

E_T^{miss} distribution of events after the three-lepton cut

Result

$W^{\pm}Z$ observed and expected events

Final State	$eee + \not{E}_T$	$ee\mu + \not{E}_T$	$e\mu\mu + \not{E}_T$	$\mu\mu\mu + \not{E}_T$
Observed	2	2	2	6
Expected $W^{\pm}Z$	1.32 ± 0.09	1.76 ± 0.10	2.48 ± 0.11	3.52 ± 0.13
Backgrounds:				
ZZ	0.03 ± 0.03	0.12 ± 0.01	0.08 ± 0.01	0.18 ± 0.01
W/Z+jets	0.09 ± 0.02	0.17 ± 0.04	0.24 ± 0.07	0.52 ± 0.08
Top	–	0 ± 0.03	–	0.35 ± 0.18
Total Background	0.25 ± 0.14	0.29 ± 0.05	0.39 ± 0.10	1.05 ± 0.19

Combined Channels

Final State	Combined
Observed	12
Expected $W^{\pm}Z$	$9.08 \pm 0.22 \pm 1.26$
Backgrounds	
ZZ	$0.40 \pm 0.03 \pm 0.05$
W/Z+jets	$1.02 \pm 0.12 \pm 0.50$
Top	$0.35 \pm 0.18 \pm 0.05$
Total Background	$1.98 \pm 0.27 \pm 0.67$

Cross-Section Extraction

Total cross-section extrapolated from fiducial region:

$$\sigma_{WZ}^{tot} = 18^{+7}_{-6}(stat)^{+3}_{-3}(syst)^{+1}_{-1}(lumi) \text{ pb}$$

Fiducial cross-section:

$$\sigma_{WZ}^{fid} = 6.6^{+2.5}_{-2.1}(stat)^{+1.1}_{-1.0}(syst)^{+0.4}_{-0.4}(lumi) \text{ pb}$$

Measurement of the W^+W^- cross-section

CERN-PH-EP-2011-054

- Using ATLAS data recorded in 2010 with $\sqrt{s} = 7$ TeV corresponding to 34 pb^{-1}

Selection cuts

- Single electron or muon trigger
- Exactly two well-reconstructed oppositely charged leptons
- For leptons with same flavour: $|m_{ll} m_Z| < 10 GeV$ and $m_{ll} > 15$ GeV to exclude resonances
- $E^{\mathrm{miss}}_{\mathrm{T,rel}} > 40 GeV$ for leptons with same flavour, $E^{\mathrm{miss}}_{\mathrm{T,rel}} > 20 GeV$ for different flavour
- No jets with more than $p_T > 20 GeV$ and $|\eta| < 3.0$

Main Backgrounds

- Top production
- Drell-Yan and W+jets
- Other Diboson

$$E^{\mathrm{miss}}_{\mathrm{T,rel}} = \begin{cases} E_T^{miss} \times \sin(\Delta\varphi) & \text{if } \Delta\varphi < \pi/2 \\ E_T^{miss} & \text{if } \Delta\varphi \geq \pi/2 \end{cases}$$

W^+W^- observed and expected Events

Final State	$e^+e^-E_{\mathrm{T,rel}}^{\mathrm{miss}}$	$\mu^+\mu^-E_{\mathrm{T,rel}}^{\mathrm{miss}}$	$e^{\pm}\mu^{\mp}E_{\mathrm{T,rel}}^{\mathrm{miss}}$
Observed Events	1	2	5
Expected W^+W^-	$0.79 \pm 0.02 \pm 0.09$	$1.61 \pm 0.04 \pm 0.14$	$4.45 \pm 0.06 \pm 0.44$
Backgrounds			
Drell-Yan	$0.00 \pm 0.10 \pm 0.07$	$0.01 \pm 0.10 \pm 0.07$	$0.22 \pm 0.06 \pm 0.15$
WZ, ZZ, $W\gamma$	$0.05 \pm 0.01 \pm 0.01$	$0.10 \pm 0.01 \pm 0.01$	$0.23 \pm 0.05 \pm 0.02$
W+jets	$0.08 \pm 0.05 \pm 0.03$	$0.00 \pm 0.29 \pm 0.10$	$0.46 \pm 0.12 \pm 0.17$
Top	$0.04 \pm 0.02 \pm 0.02$	$0.14 \pm 0.06 \pm 0.07$	$0.35 \pm 0.10 \pm 0.19$
Total Background	$0.17 \pm 0.11 \pm 0.08$	$0.25 \pm 0.31 \pm 0.15$	$1.26 \pm 0.17 \pm 0.31$

Cross-Section Measurement

The Cross-Section is determined by a maximum-likelihood fit combining the three channels. The resulting cross-section is $\sigma_{W^+W^-} = 41^{+20}_{-16}(stat) \pm 5(syst) \pm 1(lumi)$ pb

Combined Channels

Final State	Combined
Observed Events	8
Expected W^+W^-	$6.85 \pm 0.07 \pm 0.66$
Backgrounds	
Drell-Yan	$0.23 \pm 0.15 \pm 0.17$
WZ, ZZ, $W\gamma$	$0.38 \pm 0.04 \pm 0.04$
W+jets	$0.54 \pm 0.32 \pm 0.21$
Top	$0.53 \pm 0.12 \pm 0.28$
Total Background	$1.68 \pm 0.37 \pm 0.42$

Summary of Measurements

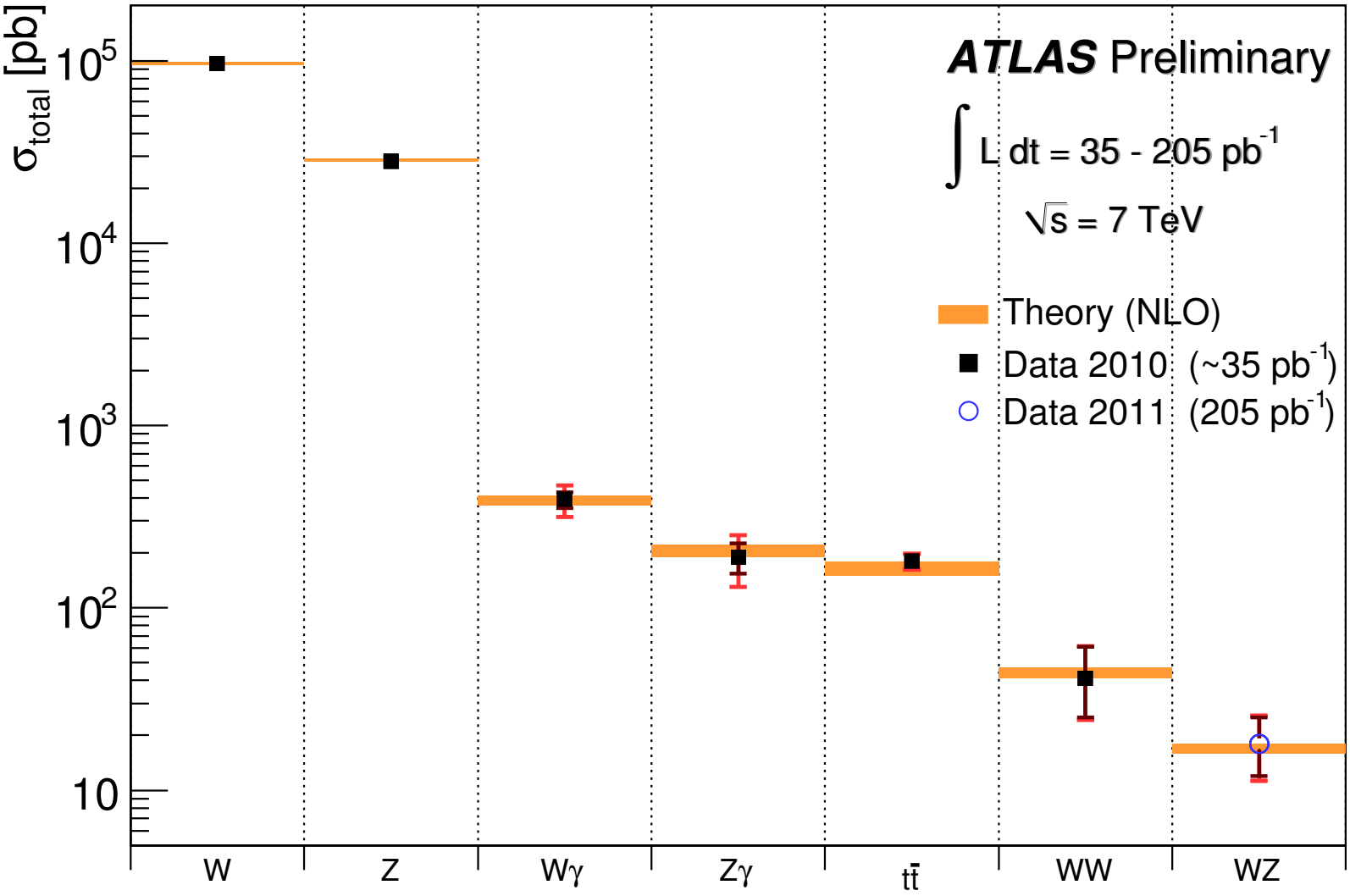

Outlook

- update cross-section measurements with 2011 data
- set limits on anomalous triple-gauge couplings

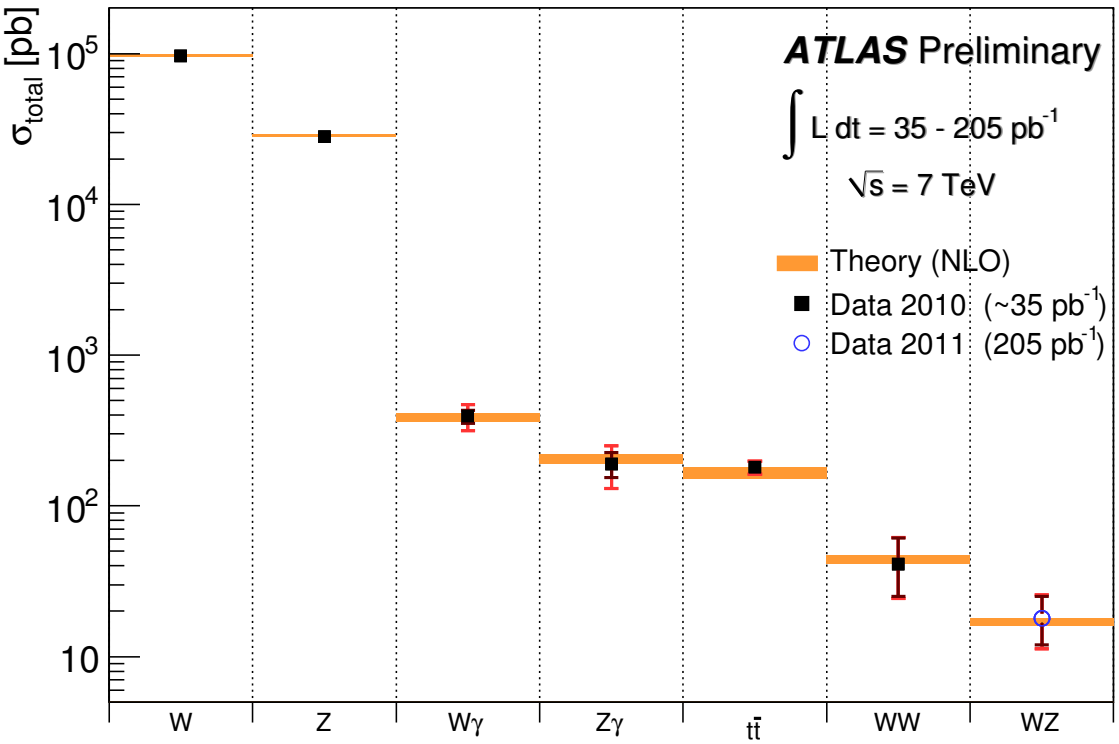

Bonus Slides

Main Systematic Uncertainties

- definition of non-tight control sample in fit
- statistical precision of fake factors and efficiencies in the weight matrix
- method used to derive identification efficiencies
- knowledge of material in front of the ECAL

Measurement of differential $\gamma\gamma$ cross-section

Acceptance Region

- Require two photons with
  - transverse momentum $p_T^{\gamma} > 16$ GeV
  - and $|\eta^{\gamma}| < 2.37$
  - ..but excluding $1.37 < |\eta^{\gamma}| < 1.52$ (barrel-endcap transition)
- The separation of the two photons must be $\Delta R_{\gamma\gamma} > 0.4$
- Both photons must be isolated: The transverse energy flow in a cone of angular radius $R < 0.4$ must be $E_T^{iso(part)} < 4$ GeV

Experimental Selection

- "Tight" photon selection
- Isolation transverse energy $E_T^{iso} < 3$ GeV

Isolation transverse energy

+ sum ECAL and HCAL cells surrounding the photon

- subtract central core with most of the photon E_T

% correct out-of-core energy

- subtract ambient energy correction from soft jets and in-time pileup

Differential cross-section $d\sigma/d\Delta\varphi_{\gamma\gamma}$

Error bars

The error bars show the total uncertainty, the statistical contribution is marked in red.
The hatched bands display the NLO computations by DIPHOX and ResBos.

Conclusion

Spectrum broader towards low values of $\Delta\varphi_{\gamma\gamma}$ than NLO predictions. Similar effects also observed at the TeVatron.

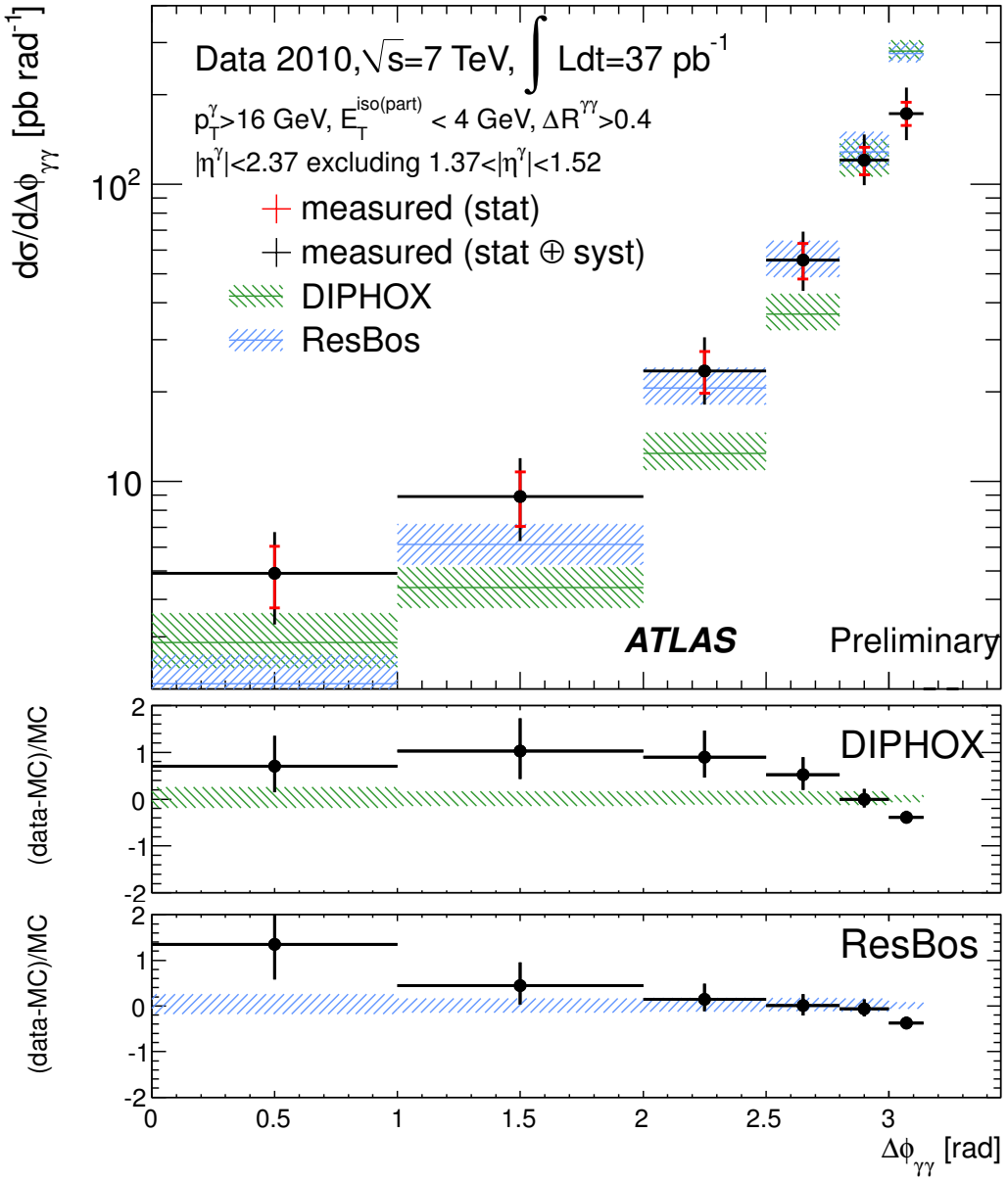

Differential cross-section $d\sigma/dm_{\gamma\gamma}$

Error bars

The error bars show the total uncertainty, the statistical contribution is marked in red.
The hatched bands display the NLO computations by DIPHOX and ResBos.

Conclusion

Good agreement with both predictions, except in low mass region - related to $\Delta\varphi_{\gamma\gamma}$ discrepancy.

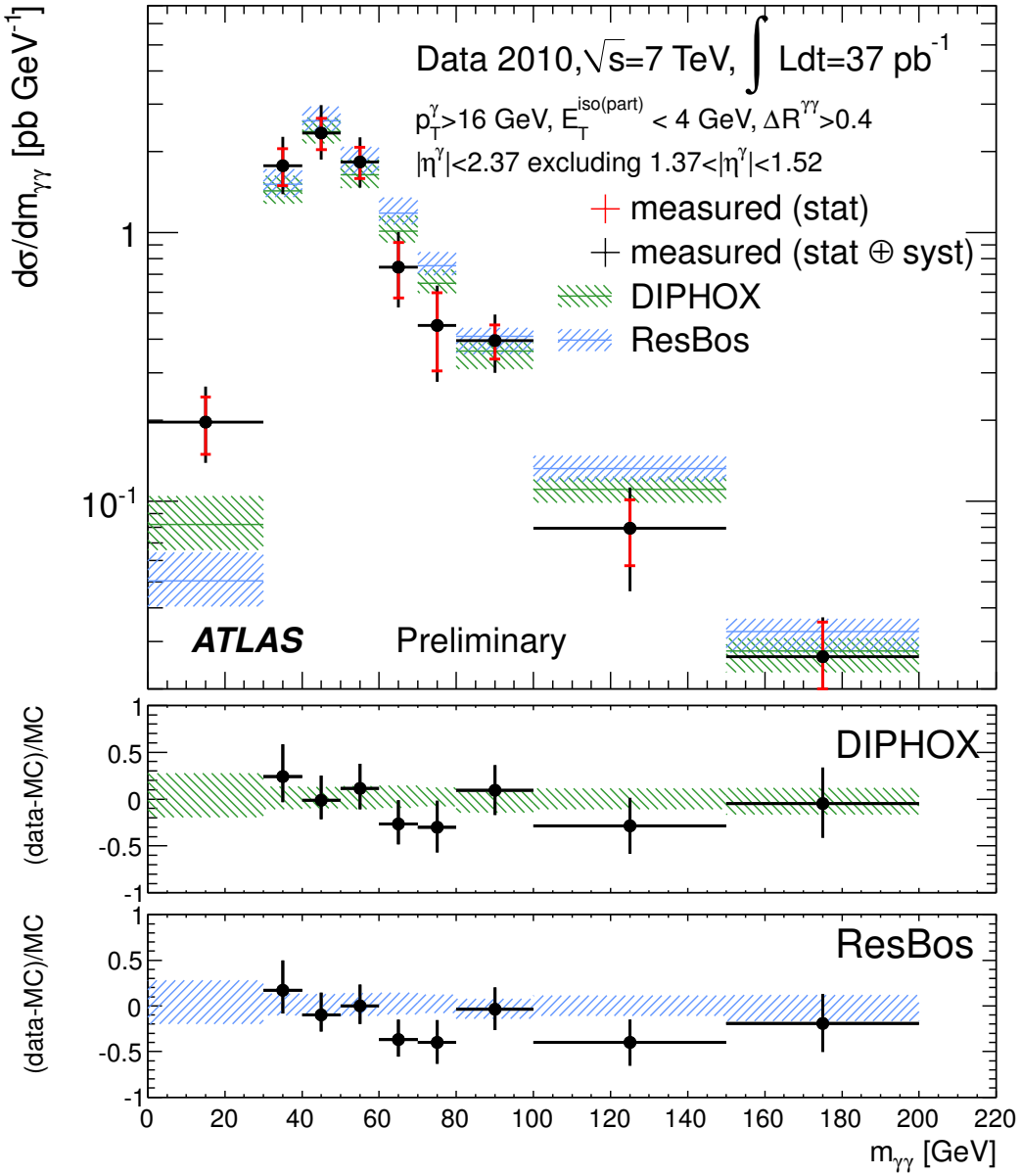

Differential cross-section $d\sigma/dp_{T_{\gamma\gamma}}$

Error bars

The error bars show the total uncertainty, the statistical contribution is marked in red.
The hatched bands display the NLO computations by DIPHOX and ResBos.

Conclusion

Generally good agreement with both predictions, except in the region between 50 GeV and 60 GeV

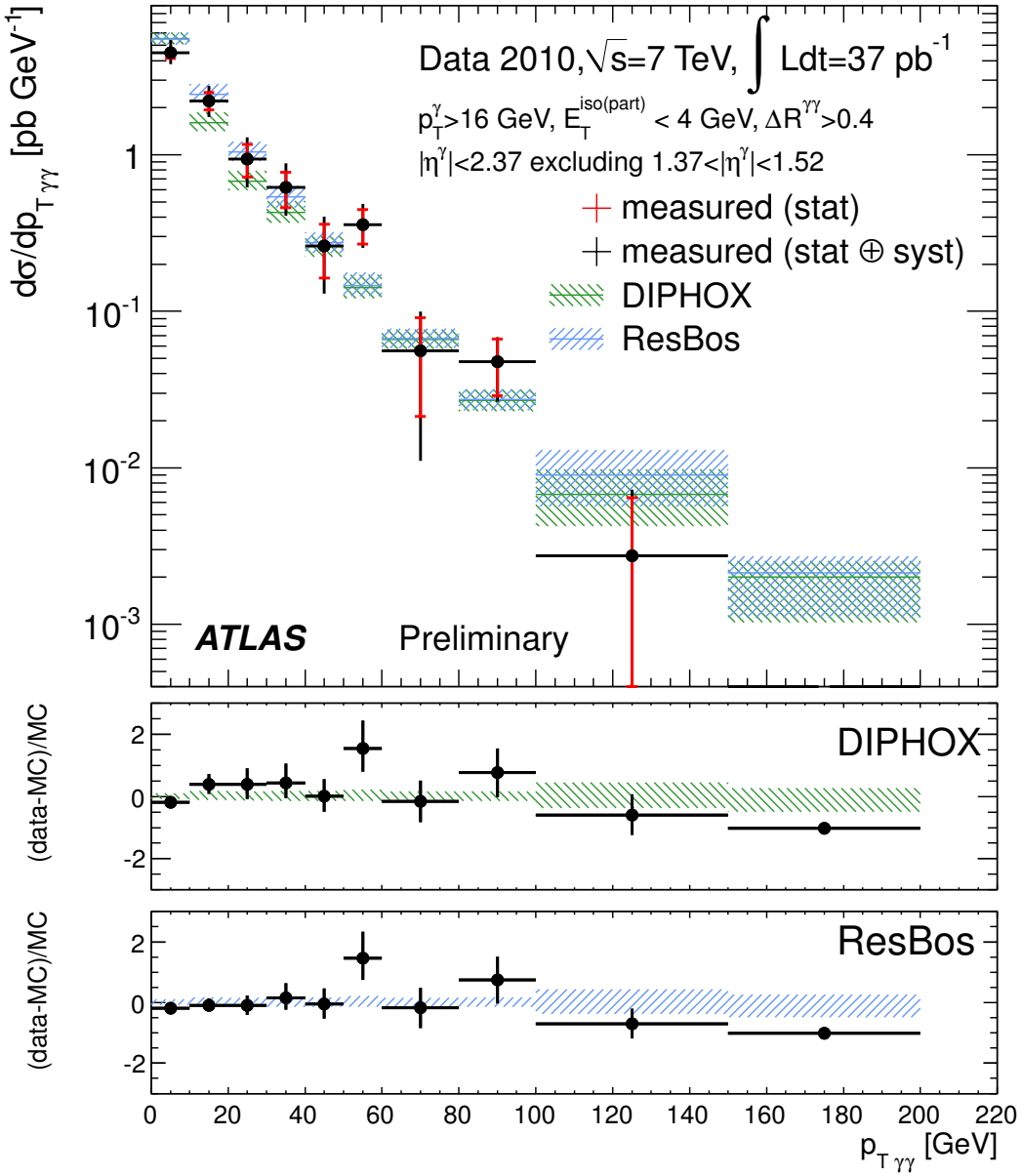

Di-photon event display

Event with high $m_{\gamma\gamma}$ showing a conversion in the leading photon

Details

$m_{\gamma\gamma} = 188.8$ GeV
$p_{T,1} = 94.5$ GeV
$p_{T,2} = 83.0$ GeV
$E_{T,1}^{iso} = 2133$ MeV
$E_{T,2}^{iso} = 1208$ MeV

Conversion

$R_{conv} = 131.1$mm
$p_{T,conv} =$ 50.2/39.2 GeV

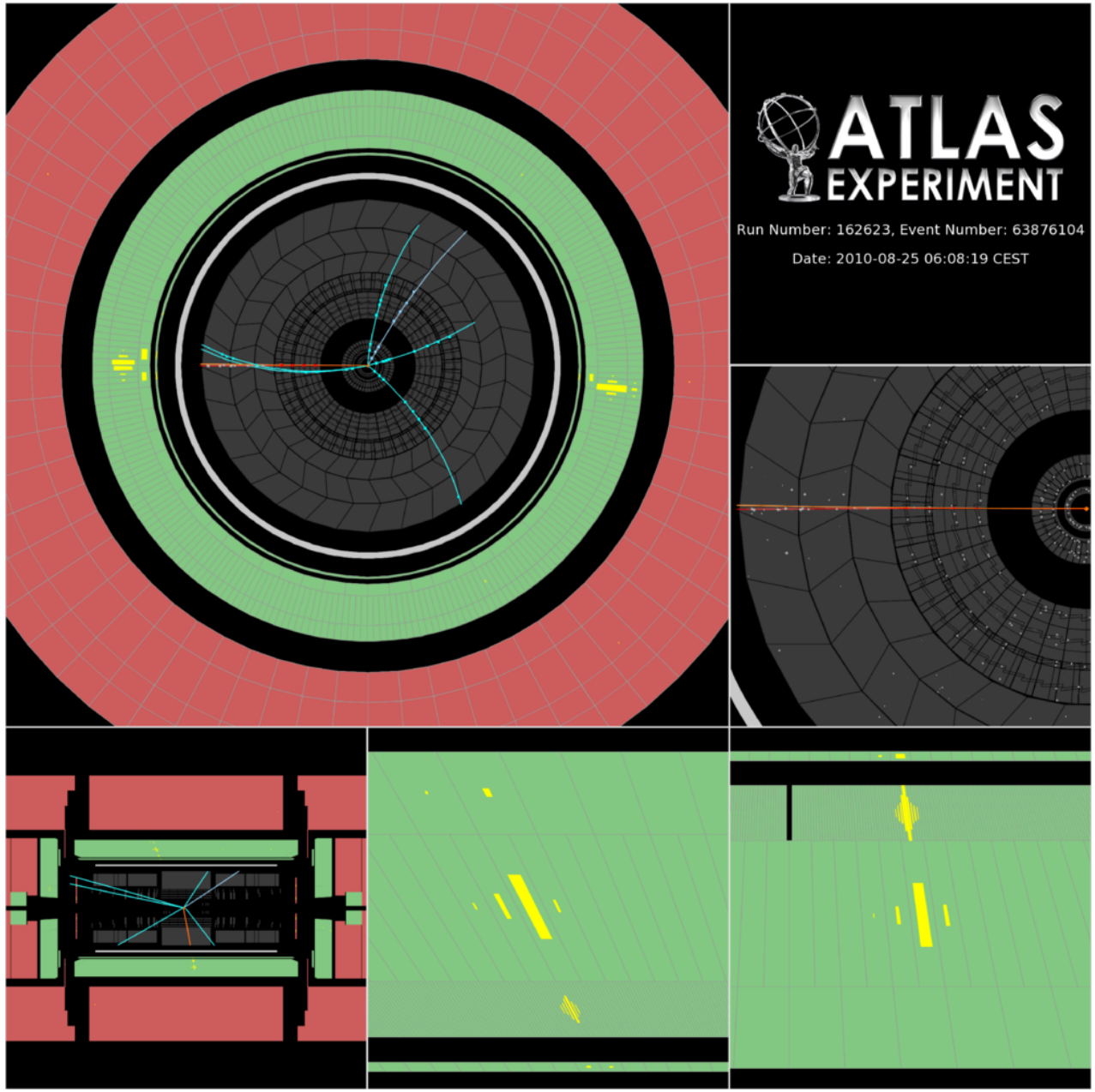

Di-photon event display

Event with small $\Delta\varphi_{\gamma\gamma}$ and an additional jet in the EndCap (shown on the right)

Details

$m_{\gamma\gamma} = 143.1$ GeV
$\Delta\varphi_{\gamma\gamma} = 1.53$
$p_{T,1} = 93.3$ GeV
$p_{T,2} = 72.8$ GeV
$E_{T,1}^{iso} = -790$ MeV
$E_{T,2}^{iso} = -1630$ MeV

$W\gamma$ DISTRIBUTIONS

Photon Transverse Energy

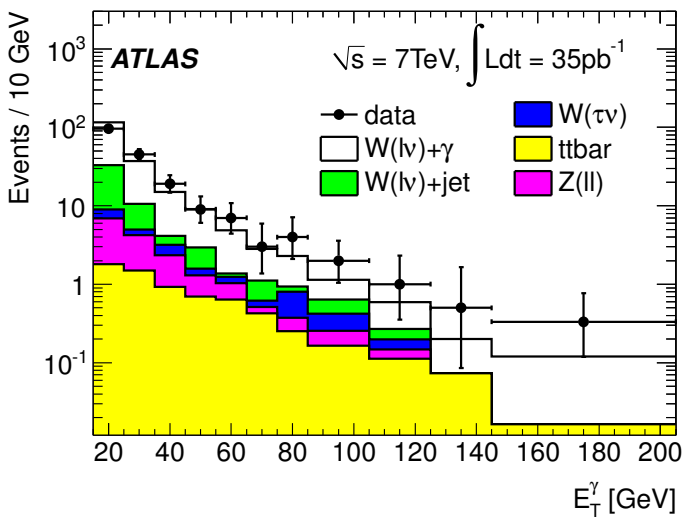

Lepton-Photon ΔR

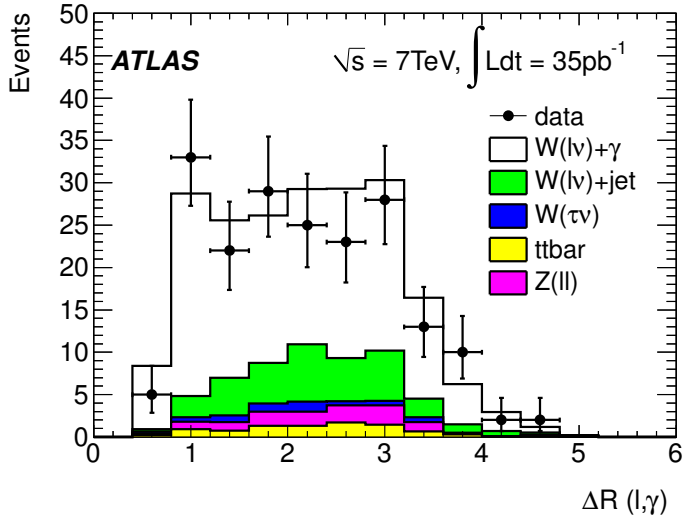

$W\gamma$ DISTRIBUTIONS

LEPTON-E_T^{miss} TRANSVERSE MASS

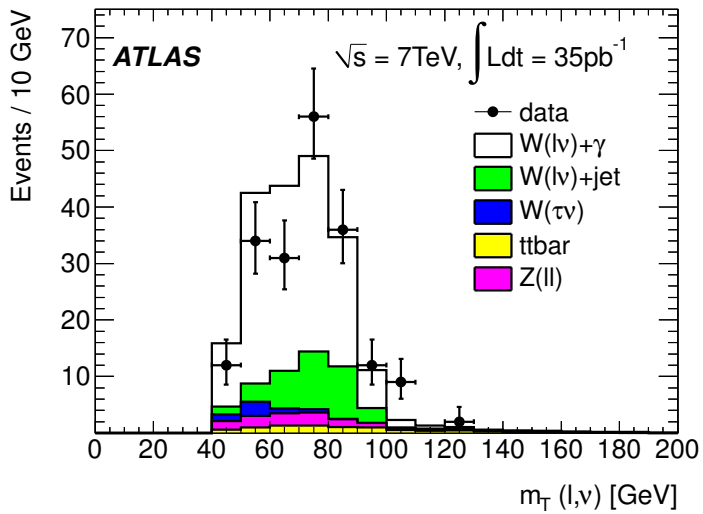

THREE-BODY INVARIANT MASS

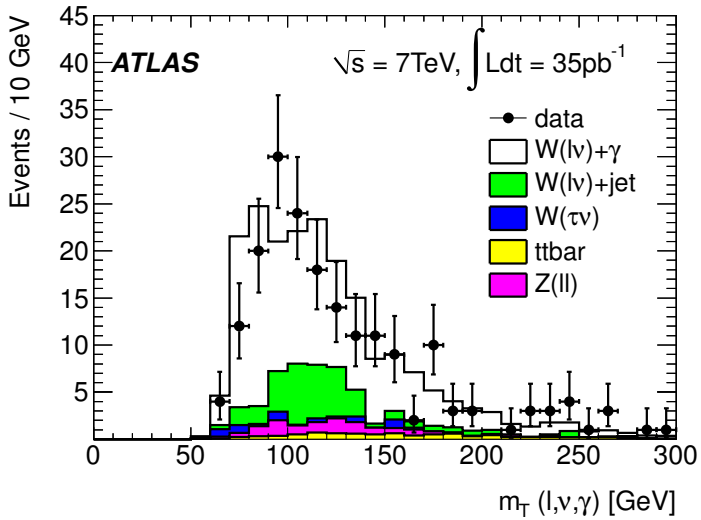

$Z\gamma$ DISTRIBUTIONS

THREE-BODY INVARIANT MASS

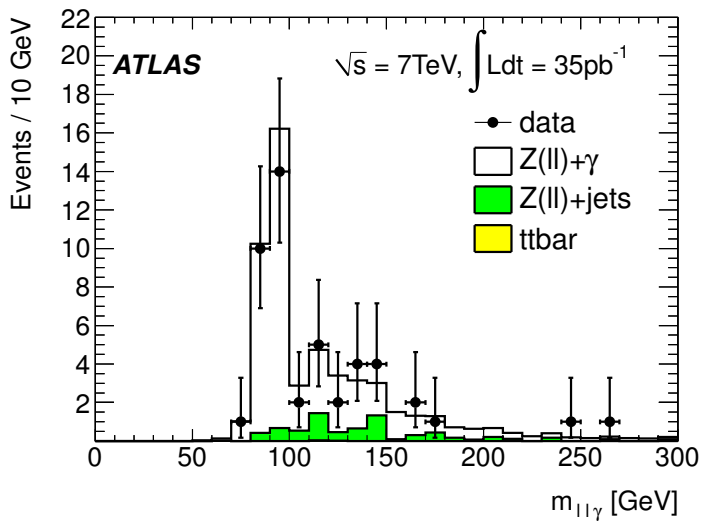

INVARIANT MASS $m_{ll}/m_{ll\gamma}$

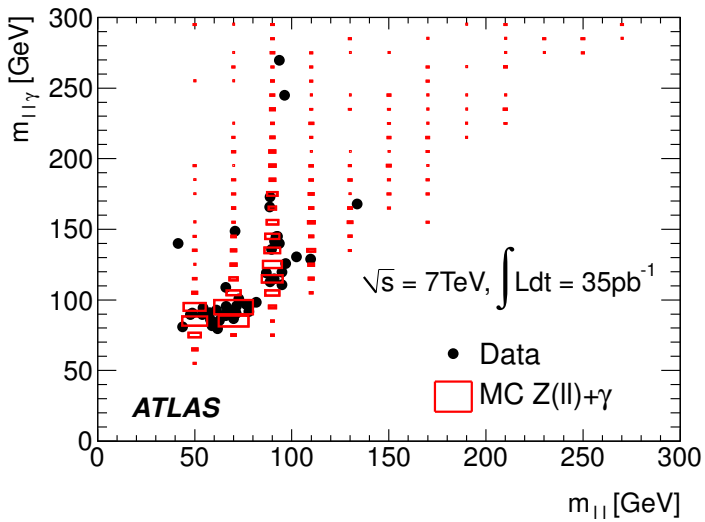

Observations of $W\gamma$

Process	Observed	EW+tt	W+jets	Extracted Signal
$W\gamma \to e^{\pm}\nu\gamma$	95	$10.3 \pm 0.9 \pm 0.7$	$16.9 \pm 5.3 \pm 7.3$	$67.8 \pm 9.2 \pm 7.3$
$W\gamma \to \mu^{\pm}\nu\gamma$	97	$11.9 \pm 0.8 \pm 0.8$	$16.9 \pm 5.3 \pm 7.4$	$68.2 \pm 9.3 \pm 7.4$

Observations of $W\gamma$

Process	Observed	EW+tt	Extracted Signal
$Z\gamma \to e^{+}e^{-}\gamma$	25	3.7 ± 3.7	$21.3 \pm 5.8 \pm 3.7$
$Z\gamma \to \mu^{+}\mu^{-}\gamma$	23	3.3 ± 3.3	$19.7 \pm 4.8 \pm 3.3$

Conclusion

While the current measurements are not strongly sensitive to possible new physics, the distributions of kinematic variables determined from the leptons and photons are consistent with the predictions from the SM in a new kinematic regime, as is the ratio of the $W\gamma/Z\gamma$ cross sections, which directly depends upon the values of the TGCs in the Standard Model.

Initial Selection Plots

$E_{\mathrm{T,rel}}^{\mathrm{miss}}$ for ee and $\mu\mu$ events

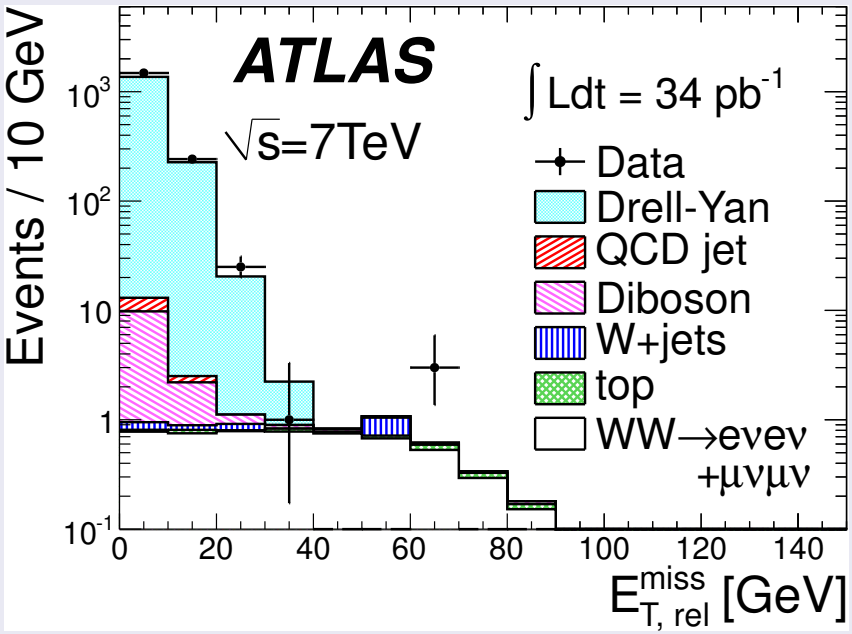

Jet Multiplicity

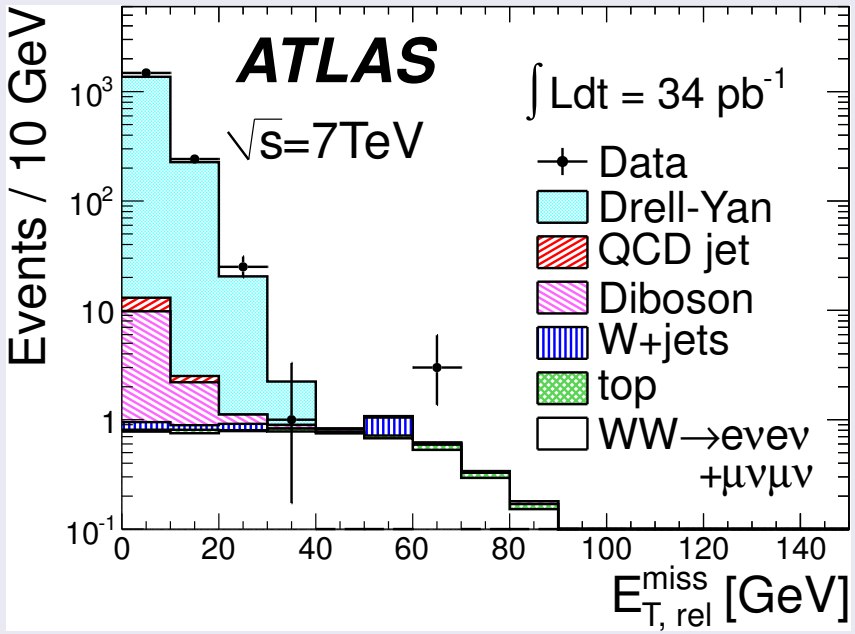

jets ($p_T > 20$ GeV and $|\eta| < 3.0$)

Relative missing transverse energy $E_{\mathrm{T,rel}}^{\mathrm{miss}}$

$$E_{\mathrm{T,rel}}^{\mathrm{miss}} = \begin{cases} E_T^{miss} \times \sin(\Delta\varphi) & \text{if } \Delta\varphi < \pi/2 \\ E_T^{miss} & \text{if } \Delta\varphi \geq \pi/2 \end{cases}$$

W^+W^- Candidate Plots

Dilepton System p_T

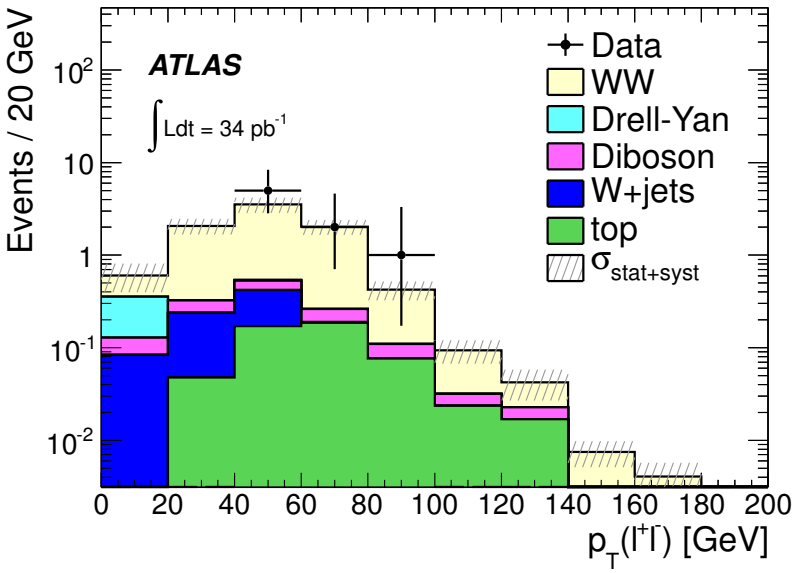

Distributions of dilepton system p_T for W^+W^- candidates

Azimuthal Angle

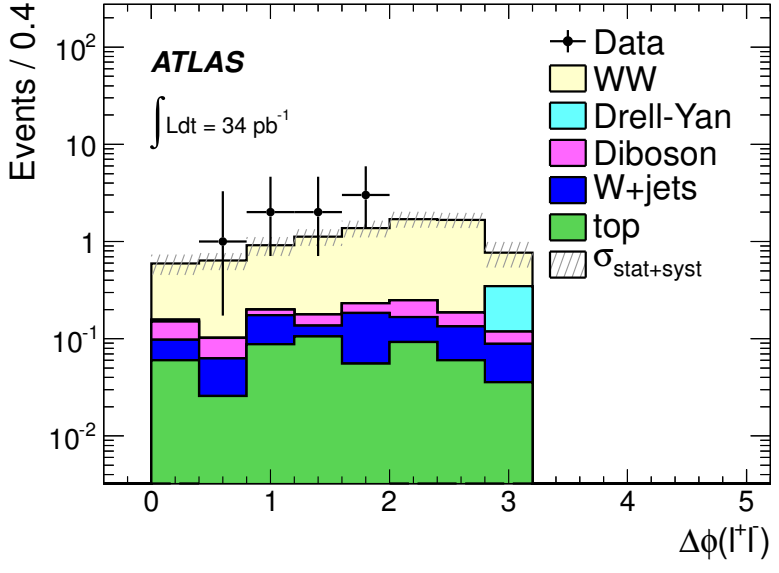

Distributions of the azimuthal angle $\Delta\varphi_{ll}$ between the leptons for W^+W^- candidates.